Keldysh Institute of Applied Mathematics
Russian Academy of Sciences

E.I. Kugushev, E.E. Pirogova, E.L. Starostin

A mathematical model of three-dimensional structure formation of RNA

Moscow 1998

Abstract. The paper deals with a mathematical model of three dimensional structure of RNA molecule which is described as a thin elastic rod. Presented are the first results of numerical identification of parameters of the model on the basis of experimental free energy characteristics of spatial element structures of RNA: hairpin, interior and bulge loops.

Key words: mathematical modelling, three-dimensional structure of RNA, tertiary structure of RNA.

Contents

1 Introduction

The spatial shape of a biological molecule is known to be one of the important determinants of its biochemical properties. Therefore, specification of three-dimensional folding of biological macromolecules from their chemical formulas is now one of the most challenging fundamental problems of molecular biology. This work is devoted to the search of methods of solution to this problem for an important type of biopolymers, ribonucleic acids (RNAs).

From the viewpoint of energetically most strong bonds, the RNA structure may be described hierarchically. First of all, there is a primary structure of a molecule. The primary structure describes the molecule as a chain of nucleotides which are linked sequentially by the strongest phosphodietheric bonds. Some nucleotides in this chain are linked in pairs by the so-called Watson-Crick bonds, which are strong enough, too. The structure of these bonds is called the secondary structure of RNA. Because of the finiteness of the set of all possible Watson-Crick bonds, the number of secondary structures, which given molecule may form, is also finite but it is rather big. Determination of real secondary structure of RNA from its primary structure is another important fundamental problem of molecular biology. By a tertiary structure of a RNA molecule is meant a three-dimensional shape which is taken by its molecular chain in space under the Watson-Crick and other weaker potentials.

In this paper, we do not consider the problem of determination of the secondary structure of RNA which is assumed to be known. Therefore, the problem is stated as computation of the tertiary structure of a RNA molecule knowing its secondary structure.

A mathematical model of such an object may be built at least at three possible levels of details.

1) An atomic model that describes an RNA molecule as a set of coordinated atoms with specified atomic interaction potentials.

2) A nucleotide model in which an RNA molecule is described as a multi-joint, each link of which is a nucleotide. The joints corresponding to linear (phosphodietheric) and cross-bonds have their own potentials. Note that other potentials describing weaker interatomic influence in a molecule can be taken into consideration.

3) A continuous model that describes an RNA molecule as an elastic rod with elastic cross-bonds. As in the nucleotide model, additional potentials can be introduced characterizing weaker interactions between atoms in a molecule. In the simplified continuous model the cross-bonds are treated as absolutely rigid.

Each of the above models has its own advantages and drawbacks. At the first stage of the investigation, we concentrated our attention on the continuous model keeping in mind that it may serve as an initial step for construction of the more detailed models. Within the framework of this model, a molecular chain is considered as a thin elastic rod with cross-bonds. On an appropriate choice of the parameters of the rod, its three-dimensional shape describes approximately the spatial configuration of the RNA molecule. Note that the continuous model has become traditional in studies of three-dimensional shapes of the DNA molecules [1]. This is partially explained by the fact that the effective coefficients of elasticity of the DNA chain were determined in experiment. Corresponding data for RNA are unknown though they are the correct values of the parameters of the model that predetermine the mathematical modelling to be adequate. Therefore, as a first aim, we formulate a problem of identification of the elastic rod parameters in the continuous model describing the spatial structure of RNA.

2 Equilibrium equations of thin elastic rod

The classical equations of the equilibrium of a thin elastic rod [2] include 6 parameters: two bending and one twisting stiffness coefficients A, B, C; the configuration parameters p_0, q_0, r_0, specifying the geometry of the rod in the relaxed state (the projection of the curvature and the twist on the principal axes of the strain tensor). The principal axes of the strain constitute a principal trihedral. Let s be the length measured along the axial line of the rod and denote $\vec{\omega}(s)$ a vector of the angular velocity of rotation of the principal trihedral as it moves along the central axis. This vector may be projected on the principal axes of the strain tensor: $\vec{\omega}(s) = (p, q, r)$. We can then write [2] for a rod under end forces only

$$\begin{aligned}
&Ap' = Br(q - q_0) - Cq(r - r_0) + F_2,\\
&Bq' = Cp(r - r_0) - Ar(p - p_0) - F_1,\\
&Cr' = Aq(p - p_0) - Bp(q - q_0),\\
&F_1' = rF_2 - qF_3,\\
&F_2' = pF_3 - rF_1,\\
&F_3' = qF_1 - pF_2,
\end{aligned} \tag{2.1}$$

where $\vec{F} = (F_1, F_2, F_3)$ is the concentrated force vector, which is applied to the first end of the rod, its components are projections on the principal axes of strain of the rod, and prime means the derivative with respect to contour parameter s.

The elastic energy of the rod is

$$G = \frac{1}{2}\int_0^L A(p - p_0)^2 + B(q - q_0)^2 + C(r - r_0)^2 ds, \qquad (2.2)$$

where S is the total length of the rod.

Note the scaling property of the model described. Consider two rods which only differ by their elastic parameters. Let they be A, B, C for the first rod, and, respectively, $\lambda A, \lambda B, \lambda C$ for the second one, where $\lambda > 0$ is a constant. Now we apply the point force $\vec{F} = (F_1, F_2, F_3)$ to the first rod, and the force $\lambda\vec{F} = (\lambda F_1, \lambda F_2, \lambda F_3)$ to the second one. Then the above system of equations (2.1) has identical solutions for identical initial values of the angular velocity of rotation of the principal trihedral $\vec{\omega}(0)$, i.e. the both rods will take the same shape in space. And the elastic energy will be equal to G for the first rod and λG for the second one.

3 Elements of a secondary structure of RNA

The main objective of this work is identification of the parameters of the elastic rod that is used as a continuous model of the three-dimensional structure of RNA. During the determination of these parameters we lean upon known experimental data. The so-called *loops*, or one-strand fragments of the RNA structure are the subject of our consideration. The loop is a sequential portion of the RNA chain where nucletotides have no Watson-Crick bonds. In contrast to the loops, the double-stranded sections are called *stems*. In stems nucleotides are joined in pairs with such bonds. It is agreed [3] that the RNA stems constitute the classical double helix structure. However, unlike DNA, which exist usually in the so-called B-form, an RNA stem takes the A-form. As compared with the B-form, the A-form has the larger diameter of its helix (23 Å instead of 19 Å), the shorter lead of the helix (28.16 Å vs. 33.8 Å) and the larger number of nucleotides per turn (11 vs. 10). The transversal bonds of the A-form do not pass through the axis of the helix and, as contrasted to the B-form, they tilt against the cross-section plane at an angle of approximately 20°. However, the length of the bonds is the same. Fig. 1(a) presents approximately 15 turns of the double-stranded fragment of RNA in the A-form.

Hairpin loops. The mentioned data make it possible, to a first approximation, to specify the boundary conditions for the so-called hairpin loop, i. e., the loop that joins the right and left strands of one stem.

In addition to the elastic rod parameters, a hairpin loop is determined by its boundary conditions, i.e. by the position and orientation of the principal trihedral in the initial (left) and in the end (right) points of the rod. As such boundary conditions we take a position and an orientation of the principal trihedral in the points of the 3' and 5' ends of the strands of the double-stranded fragment of the RNA in that place where the last Watson-Crick bond passes before the loop. We accept a simplification that the bond connects the central points of the complementary nucleotides. Thus, free rod fragments of 0.5 nucleotide length are added to the loop at its left and right ends. In particular, this means that the effective length of the hairpin loop is one nucleotide longer than nominal when the equations (2.1)–(2.2) are solved numerically. In Fig. 1(b) is presented a typical hairpin loop of 7 nucleotide length. It links the ends of the helix of the stem which is 6 nucleotide long. As the model, the "neutral" elastic rod $A = B = C$ was taken; its shape in the relaxed state (consequently, its curvature and torsion) is identical to the shape of the strands of the double-stranded fragment (stem).

Bulge loops. A bulge loop consists of two one-stranded fragments, one of which does not contain non-paired nucleotides. The length of the second fragment is called a size of the bulge loop. Fig. 2(a) shows an example of the bulge loop of 3 nucleotide long which links two stems, 6 nucleotides each.

Interior loops. An interior loop consists of two one-stranded fragments. The sizes of those fragments are parameters which define the loop. Presented in Fig. 2(b) is an example of the interior loop with lengths (1, 2) nucleotide; the loop links two stems, 6 nucleotides each.

Multibranch loops. A multibranch loop contains several (greater than two) one-stranded fragments. The number of these fragments and their lengths serve as parameters defining the loop. Fig. 2(c) shows an example of the multibranch loop of length 8 containing 4 one-stranded fragments of sizes (0, 5, 1, 2) nucleotide; the loop connects 4 stems, 4 nucleotide each.

The linking number. An important characteristic of a hairpin loop (and loops of other types) is the *linking number*, which we will denote **Lk**. Now we give its definition. A hairpin loop of RNA may be represented as a narrow *ribbon*. One edge of the ribbon $\vec{X}(s)$ coincides with the central line of the model rod. The second edge is obtained after a small shift of every point of the first edge along the Watson-Crick bond direction. The last is interpolated in-between adjacent nucleotides to form a continuous generalization and it is denoted by $\vec{U}(s)$. Then the edges of the ribbon may be given in the form $\vec{X}(s)$ and $\vec{X}(s) + \epsilon\vec{U}(s)$. The width of the ribbon is assumed to be sufficiently small. Generally speaking, a ribbon may be closed, if $\vec{X}(s)$ and $\vec{U}(s)$ are periodic functions of the same period. The hairpin ribbon is formed by a single-strand fragment of the molecule between two nucleotides linked by the Watson-Crick bond.

Let us have a set of ribbons generated by hairpin loops, which correspond to fixed boundary conditions at their ends. Consider two such ribbons α and β with their central lines a and b, respectively. Let γ be a ribbon that completes α and β to closed ribbons $\alpha + \gamma$ and $\beta + \gamma$. Then the difference of the linking numbers $\delta\,\mathbf{Lk}(\alpha, \beta; \gamma)$ of α and β relative to γ is defined by

$$\delta Lk(\alpha, \beta; \gamma) = Lk(\beta + \gamma) - Lk(\alpha + \gamma),$$

where $Lk(\alpha + \gamma)$ and $Lk(\beta + \gamma)$ are the linking numbers of the closed ribbons α and β. In fact, $\delta\,\mathbf{Lk}(\alpha, \beta; \gamma)$ depends only on the shape of the central axis c of the ribbon γ [4], i.e. we can write

$$\delta Lk(\alpha, \beta; \gamma) = \delta Lk(\alpha, \beta; c),$$

where c is a spatial curve that completes the curves a and b of the ribbons α and β to closed non-self-intersecting curves $a + c$ and $b + c$. Now let us take another closing curve c'. Then

$$\delta Lk(\alpha, \beta; c) = \delta Lk(\alpha, \beta; c').$$

In other words, the difference of the linking numbers of two hairpin loops does not depend on the specific shape of the closing curve c, unless it is chosen to cross the hairpin loops.

Therefore, it is natural to define the difference of the linking numbers $\delta\,\mathbf{Lk}(\alpha,\beta)$ of the two hairpin loops α and β as a difference of the linking numbers of the two closed ribbons $\alpha+\gamma$ and $\beta+\gamma$, computed for an arbitrary closing ribbon γ that does not intersect the ribbons α and β. We may choose a particular ribbon γ_0 and fix it when carrying out computations.

Loosely defined, the linking number may be thought of as the number of turns to which the rod is twisted. If we gradually rotate the right end of the elastic rod one turn around the tangent vector then the linking number changes by $+1$ or -1 depending on the direction of the rotation. The linking number of the loop in Fig. 1(b) is equal to zero. This loop is also presented with different linking numbers $\mathbf{Lk} = -1$ (Fig. 1(c)) and $\mathbf{Lk} = +1$ (Fig. 1(d)). It may be suggested that the linking number of the loop significantly affects the biological functioning of the RNA molecule. For example, non-zero linking, for which the anticodon triplet is open to a greater extent, is preferable for the anticodon loop of the transfer RNA (tRNA).

The free energy. In our model, the free energy of an arbitrary loop is assumed to be the sum of the elastic energies of the rod which model one-stranded fragments of the loop. In particular, the free energy of a hairpin loop is assumed to be equal to the elastic energy of the model rod. The free energy of the loop also depends on its linking number. In our example, if the energy G of the loop with zero linking number is taken to equal the unity, then, for $\mathbf{Lk} = -1$, we have $G = 11.26$ and $G = 1.88$ for $\mathbf{Lk} = +1$. Fig. 3 represents a graph of the free energy of the hairpin loop $G(L,\psi)$ as a function of the loop length $L(3 \leq S \leq 10)$ and the angle of rotation $\psi(0 \leq \psi \leq 360°)$ of the right end of the elastic rod around its tangent vector, for the neutrally elastic rod.

4 Identification of the elastic rod parameters in the RNA model

As already noted, the main objective of this work is to identify the parameters of the elastic rod in the continuous model of RNA. The basic data for this program are experimentally obtained values of the free energy of the hairpin loop formation. Only few experimental works in this area are known. We take the data from [5] which is widely used in the current numerical investigations of the secondary structure of RNA. In that paper, the free energy is presented for RNA hairpin loops (h), 3 to 10 nucleotides long, for RNA bulge loops (b) of 1 and 2 nucleotide, and for interior loop (i) with lenghts $(1,1)$ nucleotides:

$$\begin{array}{lccccccccccccc} L & = & h3 & h4 & h5 & h6 & h7 & h8 & h9 & h10 & b1 & b2 & i(1,1) \\ G_0(L) & = & 7.4 & 5.9 & 4.4 & 4.3 & 4.1 & 4.1 & 4.2 & 4.3 & 3.3 & 5.2 & 0.8 \end{array} \tag{4.1}$$

where L is the type and the length of a loop measured in nucleotides, G_0 is its free energy in Kcal/mol.

We have found no data on the linking numbers for real hairpin loops in published works. We carry out the process of idetification of the parameters of the model elastic rod under the assumption that the experimental values of the free energy correspond to zero linking numbers. In general, this particular problem deserves further investigation.

It is also not clear for which form of stems (A or B) were the above figures obtained. Therefore, the parametric identification was carried out for both the cases.

In addition to the parameters used in (2.1): $\{A, B, C, p_0, q_0, r_0\}$, the elastic rod is characterized by a rotation angle θ of the principal axes of the strain tensor relative to the axes of the moving trihedral of the central line of the rod in its relaxed state.

For convenience of data processing, the numerical simulation was performed not using the variables $\{A, B, C, \theta, p_0, q_0, r_0\}$, but the equivalent ones $\{A, B, C, \theta, P_0, Q_0, R_0\}$. As before, the variables A, B, C are the principal two bending and one torsional coefficients of elasticity of the rod. Now explain the meaning of the rest variables (see Fig. 4). Let $\vec{r}_b$ be the starting point of the rod that models the hairpin loop. This point coincides with the $5'$ end of the corresponding chain of the double-stranded fragment of RNA that is closed by the hairpin loop. The starting boundary trihedral (or the boundary frame) is called an orthonormal frame $\{\vec{e}_{b1}, \vec{e}_{b2}, \vec{e}_{b3}\}$, which is coincident with the moving trihedral of the chain in its $5'$ end $\vec{r}_b$. The normal vector $\vec{e}_{b1}$ is directed from the point $\vec{r}_b$ to the axis line of the double helix, the tangent vector $\vec{e}_{b3}$ is directed along the tangent to the corresponding chain, and the binormal vector $\vec{e}_{b2}$ is defined as a cross product of the normal and the binormal vectors. Similarly, the end boundary trihedral $\{\vec{e}_{e1}, \vec{e}_{e2}, \vec{e}_{e3}\}$ may be introduced in the end point of the loop $\vec{r}_e$, which is coincident with the $3'$ end of the corresponding chain. The value θ is an angle of rotation of the starting boundary frame relative to the principal axes of strain around the tangent vector $\vec{e}_{b3}$. Introduce the vector $\vec{\omega}_0$, whose projections on the principal axes of strain are $\vec{\omega}_0 = (p_0, q_0, r_0)$, then (P_0, Q_0, R_0) are projections of the vector $\vec{\omega}_0$ on the axes of the starting boundary frame. The initial position of the principal trihedral may be thus found by the rotation of the starting boundary trihedral through the angle $-\theta$ around the tangent vector $\vec{e}_{b3}$. The values (p_0, q_0, r_0) are obtained as components of the vector (P_0, Q_0, R_0), rotated through the angle θ around the tangent vector. If the boundary value problem is solved exactly, then the end boundary trihedral should be obtained from the finishing position of the principal trihedral by the rotation through the angle θ around the tangent vector.

On this basis, we formulate the following problem of identification of the RNA chain parameters in the continuous model. We consider a homogeneous thin elastic rod with its ends fixed in known positions. The free energy G of this rod is the elastic energy of its bending and twisting. It may be considered as a function $G(\vec{P}, L)$, where $\vec{P}$ is the constant vector of the parameters of the rod: $\vec{P} = (A, B, C, \theta, P_0, Q_0, R_0)$, and L its length (or the lengths of its fragments) which may vary. This function value is known at a finite set of values of the length $L : G(\vec{P}, L_i) = G_0(L_i), i = 1, 2, \cdots, n$. We search for the parameter vector $\vec{P}$ such that the error functional

$$\Phi^2 = \sum_{i=1}^{n} (G(\vec{P}, L_i) - G_0(L_i))^2 \tag{4.2}$$

reaches its minimum. In our case, $n = 11$ and the values L_i $G_0(L_i)$ are given by (4.1).

The process of identification consists of two stages. At the first stage, an initial vector of the parameters is chosen $\vec{P} = \vec{Q}$ and a family of hairpin loops of length $3, 4, \cdots, 10$ nucleotides is built with zero linking number. To make this, the BVP for every loop is solved and the shape of the modelling thin elastic rod and its free energy are computed for its current parameters. This problem is solved by means of the coordinate descent in the space of initial values of the system (2.1).

At the second stage, an identification of the rod's parameters itself is performed to find such ones that give the closest approximation of the computed free energy to its experimental values for RNA hairpin loops, i.e. that minimize (4.2). The minimization process is multistep. The error functional is minimized by means of the coordinate descent in the space of the parameters $\vec{P}$. At each step, the rod's parameter values are varied and the BVP solutions are correspondingly updated for every hairpin loop from the set. We particularly emphasize that the above-mentioned (see section 2) scaling property of the BVP is exploited for acceleration of the minimization process. In fact, minimized is the error functional

$$\Psi^2(\vec{P}) = \min_{\lambda>0} \sum_{i=1}^{n} (G(\vec{P}_\lambda, L_i) - G_0(L_i))^2 \tag{4.3}$$

where $\vec{P}_\lambda = (\lambda A, \lambda B, \lambda C, \theta, P_0, Q_0, R_0)$ and $G(\vec{P}_\lambda, L_i) = \lambda G(\vec{P}, L_i)$, i. e. the parameters A, B, C are scaled by the factor λ.

5 Results of numerical experiments

We carried out one numerical experiment for A-form of RNA and another one for B-form, for initial conditions, for which the shape of the free rod is the same as the corresponding helix of A or B-form, respectively:

N_v	A	B	C	θ	P_0	Q_0	R_0
01	1	1	1	0	0.0	7.549074e-02	2.942040e−02
02	1	1	1	0	0.0	7.970578e-02	4.513392e−02

where N_v is an index of the variant.

In both cases, it was assumed that, initially, the rod has a spherical (scalar) tensor of elasticity and that it adopts either the RNA A-form helix in its free state (variant 01)

$$P_0 = 0.0, \qquad Q_0 = 7.549074e-02, \qquad R_0 = 2.942040e-02 \tag{5.1}$$

or the B-form helix (variant 02)

$$P_0 = 0.0, \qquad Q_0 = 7.970578e-02, \qquad R_0 = 4.513392e-02 \tag{5.2}$$

Fig. 5 and Fig. 6 demonstrate the secondary and tertiary experimental structures of the yeast phenylalanine transfer RNA (Phe tRNA) taken from [7]. In a scematic drawing, presented in Fig. 6, the bars between the helical backbones represent the hydrogen-bonding elements of secondary and tertiary structure. Fig. 7 shows two variants of the three-dimensional structure of this molecule obtained by using our model for parameters of the elastic rod: (5.1), A-form, Fig. 7(a) and (5.2), B-form, Fig. 7(b). For all pictures of the three-dimensional shape of the molecule, the view direction is chosen perpendicular to the molecular plane. One might notice a similarity of the experimental and model structures. However, variant 02 (Fig. 7(b)) seems to be preferable. The model captures the following important features of the overall tracing of the polynucleotide chain as it was revealed by means of an X-ray diffraction study [7]:

- the molecule as a whole is somewhat flattened;
- it has an L-shape conformation;
- the acceptor stem (at the upper right corner of the figures)

approximately has right angle to the anticodon stem (at the bottom);

- the two other stems are in the position that facilitates the tertiary interactions between nucleotides of their hairpin loops.

The process converged to a local minimum of the error functional for every initial condition. Below are presented the obtained data. The run index is given in the first column. The next columns contain pairs of the initial (top) and resulting (bottom) values of the error functional Ψ (4.3) and the identified parameters: A, B, C are the two bending and one torsional elasticity parameters in the principal axes, θ is the angle of rotation of the starting boundary frame relative to the principal axes of strain around the tangent vector (in radians). The parameters (P_0, Q_0, R_0) are presented in the additional part of the table. The values of the error functional and the parameters, presented in the table, correspond to measuring length in Å and energy in Kcal/mol.

N_v	Ψ	A	B	C	θ
01	2.6675	37.43998	37.43998	37.43998	$0.000000e+00$
	1.3534	12.06572	118.1943	230.4529	$-1.215676e-02$
02	2.3979	35.66384	35.66384	35.66384	$0.000000e+00$
	0.5773	38.39056	81.75962	13.76488	$7.590668e-01$

(5.3)

N_v	P_0	Q_0	R_0
01	0.0	$7.549074e-02$	$2.942040e-02$
	$1.502044e-02$	$4.323602e-02$	$3.095943e-02$
02	0.0	$7.970578e-02$	$4.513392e-02$
	$1.538353e-02$	$1.059789e-01$	$9.016210e-002$

(5.4)

All data are presented in a standard form, in which the angle θ belongs to the range $-\frac{\pi}{4} < \theta \leq \frac{\pi}{4}$. Note that interchange of indices of the cross-sectional principal axes of elasticity is equivalent to the increase or decrease of the angle R by $\pi/2$ with simultaneous interchange of the principal bending coefficients A to B or B to A. This allows us to bring all the variants to the above standard form when the first principal axis of the tensor of elasticity turns out to be the closest in its direction to the first axis of the principal trihedral.

The table (5.5) contains geometric parameters of the helix, corresponding to the central line of the elastic rod in its free state. Here k is the curvature, η the torsion, D the diameter, H the lead of the helix, L the length of one turn, N the number of nucleotides per a turn of the helix. All values are expressed in Å.

N_v	k	η	D	H	L	N
01	4.577081e-02	3.095943e-02	30.00	63.71	113.7	16.13
02	1.070896e-01	9.016210e-02	10.93	28.91	44.88	6.54

(5.5)

One can see that variant 02, corresponding to the B-form, certainly better approximates the experimental values of the free energy of the loops. Moreover, it corresponds to the data on the one-stranded structure of RNA in a crystal form, obtained in [6] by means of X-ray analysis:

	Model	Experiment
Lead of helix (Å)	28.91	18.66
Nucleotides per turn	6.54	6.0

(5.6)

In Fig. 8 one can see tertiary structures of the molecule corresponding to variants 01 (Fig. 8(a)) and 02 (Fig. 8(b)). In Fig. 9 and 10 presented are graphs of the experimental and model values of the free energy for the indicated variants.

The performed computational experiments suggest the following **conclusions**:

- the homogeneous parameters of the elastic rod, corresponding to A- or B-form, may give model three-dimensional structures close to the native ones;
- the experimental values of the free energy of RNA loops correspond more likeky to B-form.

References

[1] Benham, C. J. (1983) Geometry and mechanics of DNA superhelicity, *Biopolymers,* **22,** 11, 2477–2495.

[2] Popov, E.P. Nonlinear problems of statics of thin rods. Leningrad–Moscow, OGIZ, 1948, p.170 [in Russian].

[3] Lewin, B. (1983) *Genes,* John Wiley & Sons.

[4] Fuller, F. B. (1978) Decomposition of the linking number of a closed ribbon: A problem from molecular biology, *Proc. Natl. Acad. Sci. USA,* **75,** (8), 3557–3561.

[5] Freier, S. M., Kierzek, R., Jalger, J. A., Sugimoto, N., Caruthers, M. H., Neilson, T., and Turner, D. H. (1986) Improved free-energy parameters for predictions of RNA duplex stability, *Proc. Natl. Acad. Sci. USA,* **83**, 9373–9377.

[6] Arnott, S., Chandrasekaran, R., Leslie, A. G. W. (1976) Structure of the single-stranded polyribonucleotide polycytidylic acid, *J. Mol. Biol.,* **106,** 735–748.

[7] Kim, S. H., Suddath, F. L., Qugley, G. J., McPherson, A., Sussman, J. L., Wang, A. H. J., Seeman, N. C., Rich, A. (1974) Three-dimensional tertiary structure of yeast phenylalanine transfer RNA, *Science,* **185,** N 4149, 435–440.

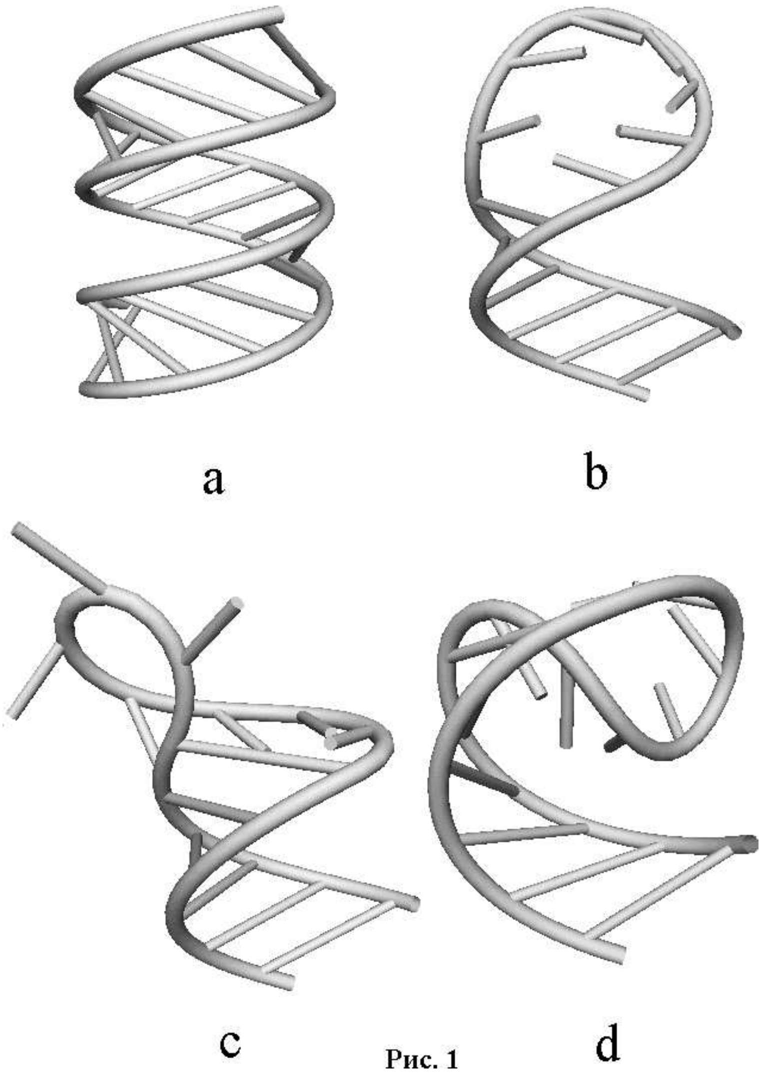

Figure 1: Hairpin loops.

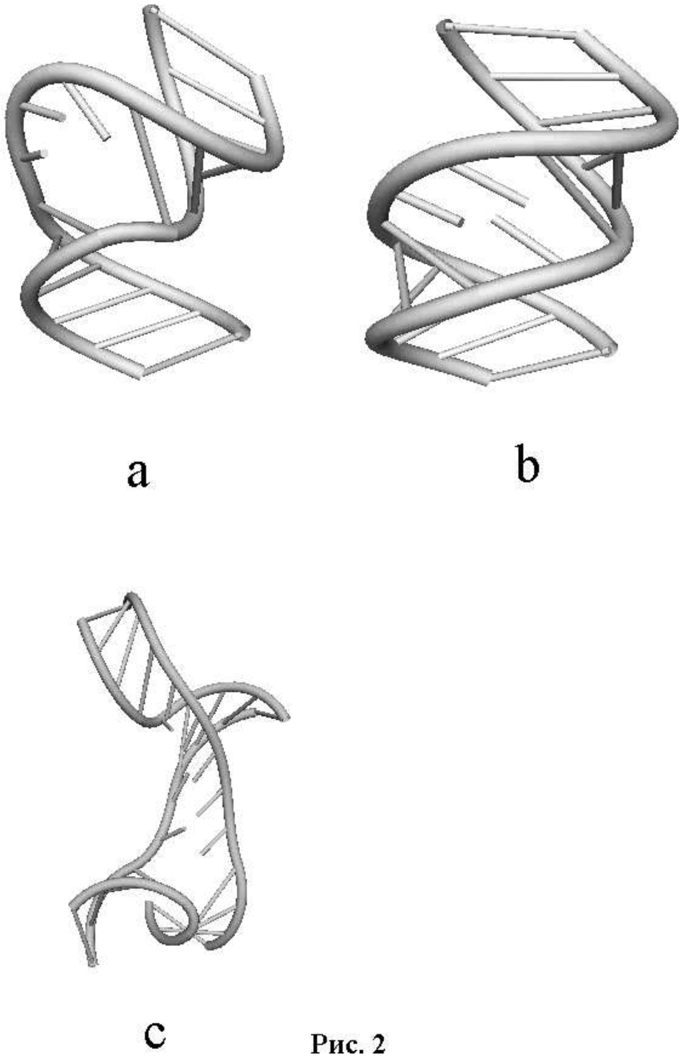

Рис. 2

Figure 2: Loops types.

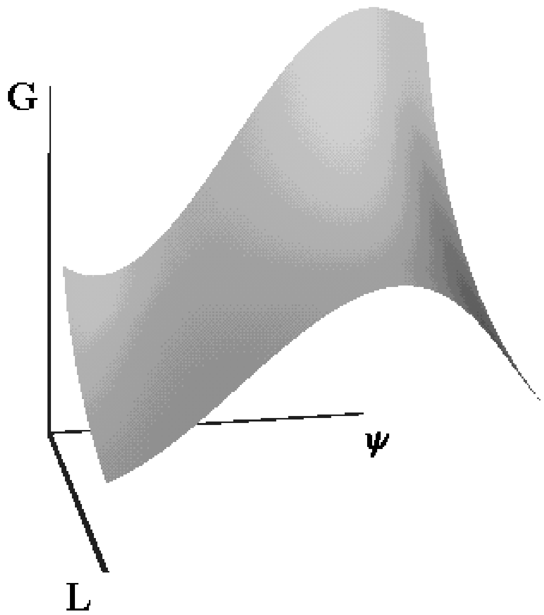

a

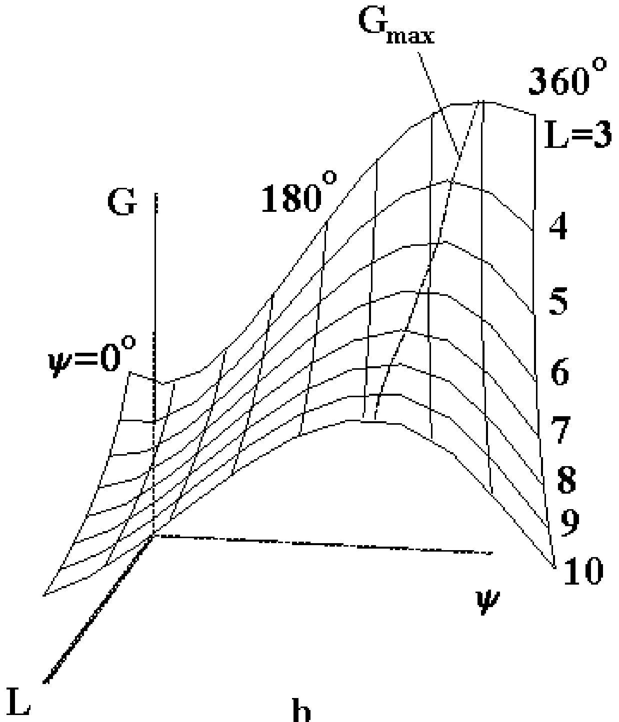

b

Рис. 3

Figure 3: Free energy.

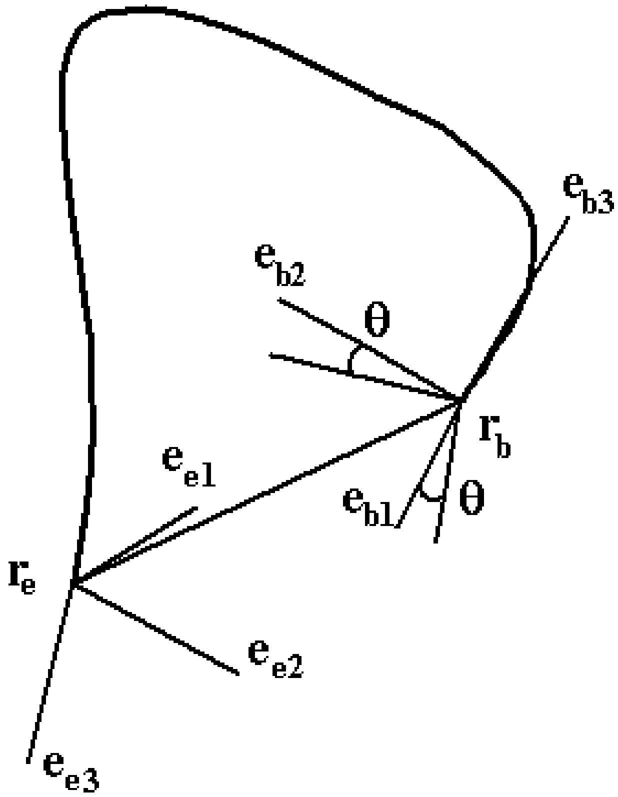

Рис. 4

Figure 4: The starting and end trihedrals.

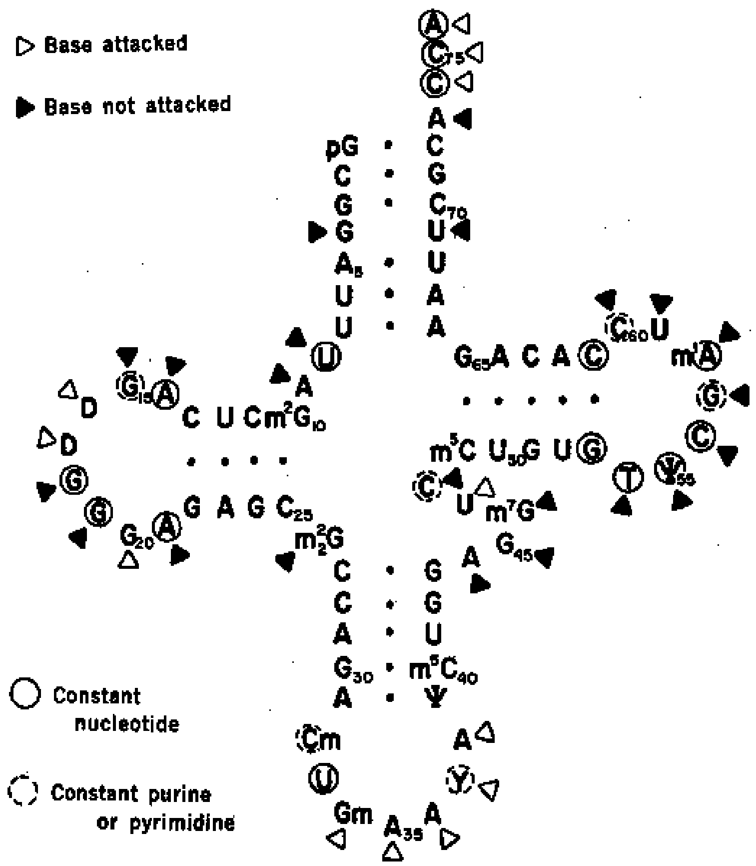

Рис. 5a

Figure 5: The secondary structure of Phe tRNA.

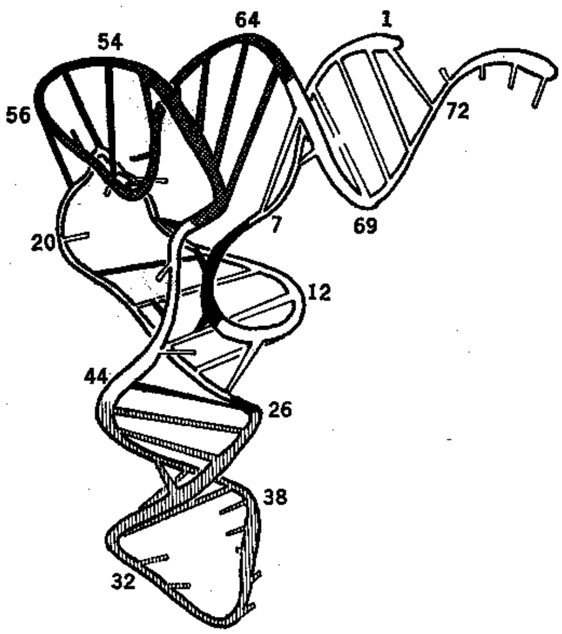

Рис. 5b

Figure 6: The tertiary structure of Phe tRNA. The ribose phosphate backbone is drawn as a continuous cylinder with bars to indicate the Watson-Crick-bonded nucleotides. The anticodon stem and hairpin loop are marked by vertical lines.

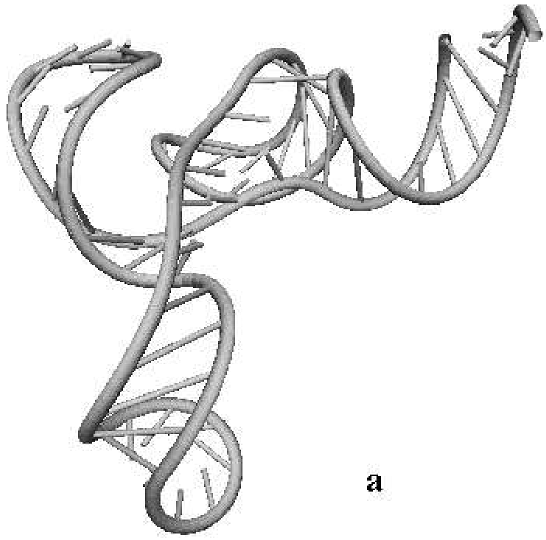

a

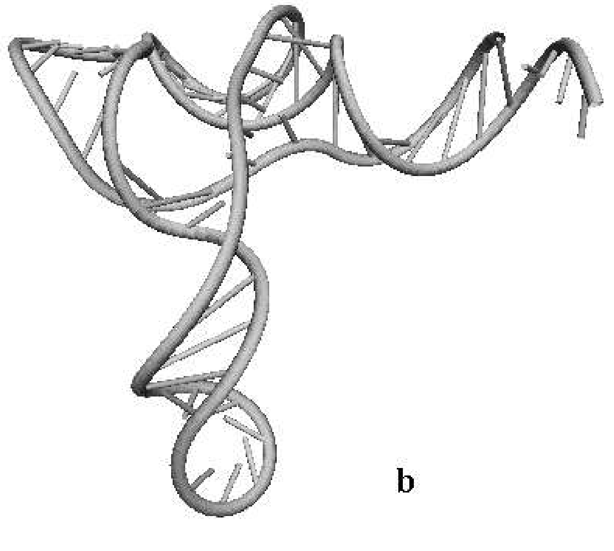

b

Рис. 6

Figure 7: The three-dimensional structure of Phe tRNA.

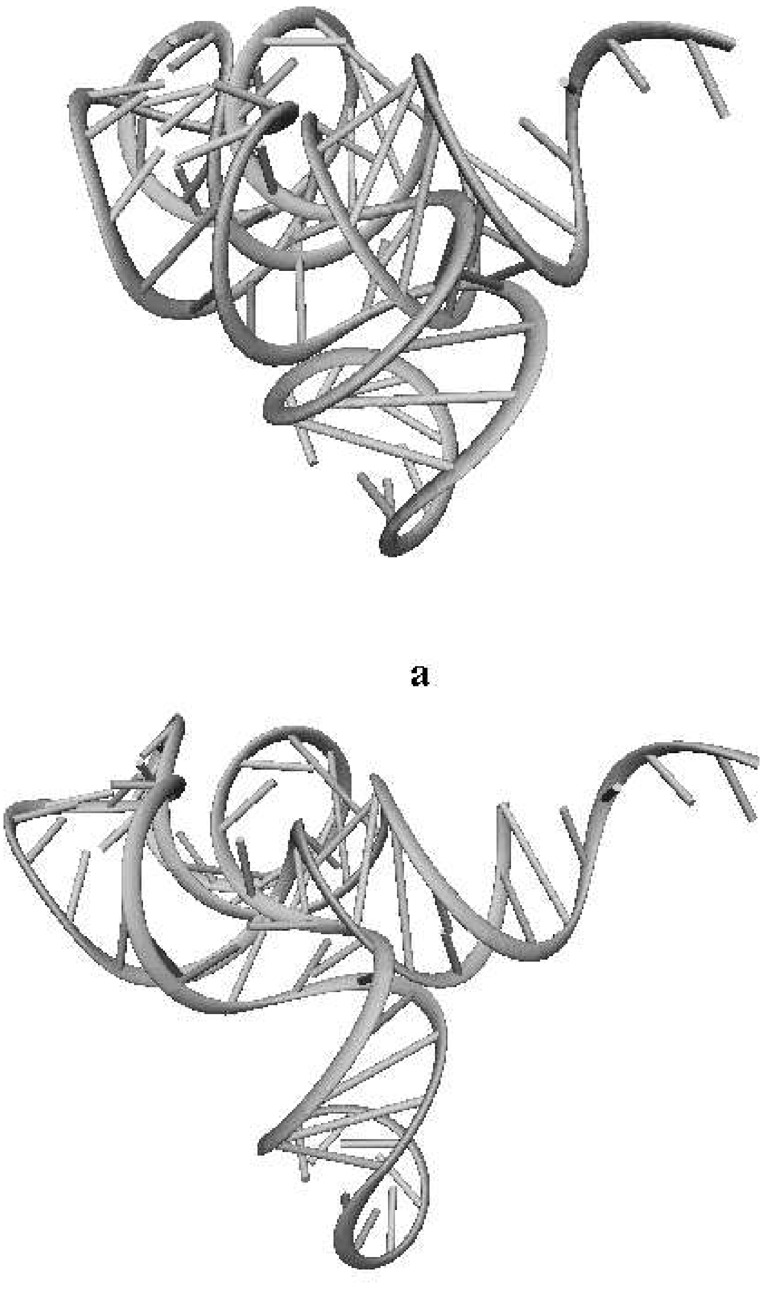

a

b

Рис. 7

Figure 8: The three-dimensional structure of Phe tRNA for two variants.

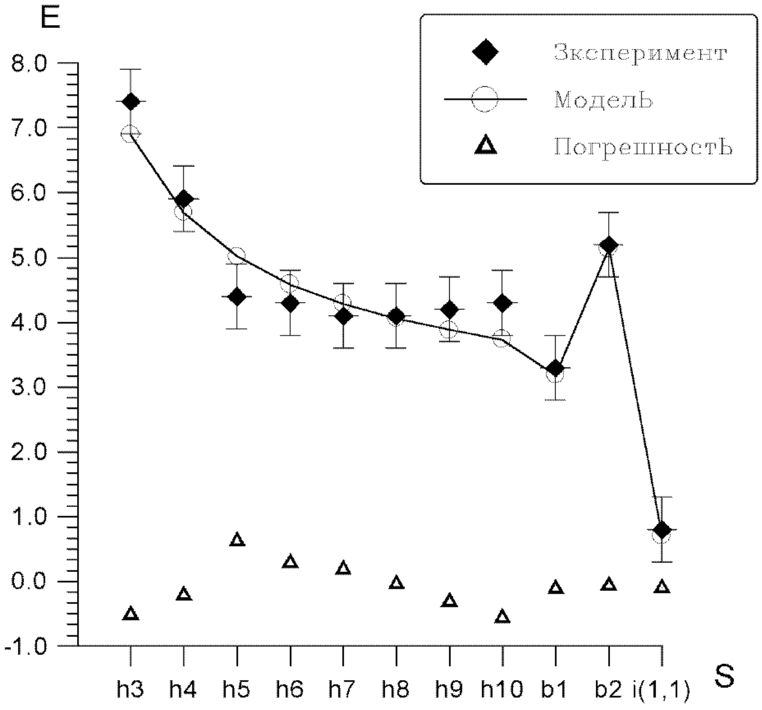

Рис. 8а

Figure 9: Comparison between experimental and model energy (variant 01).

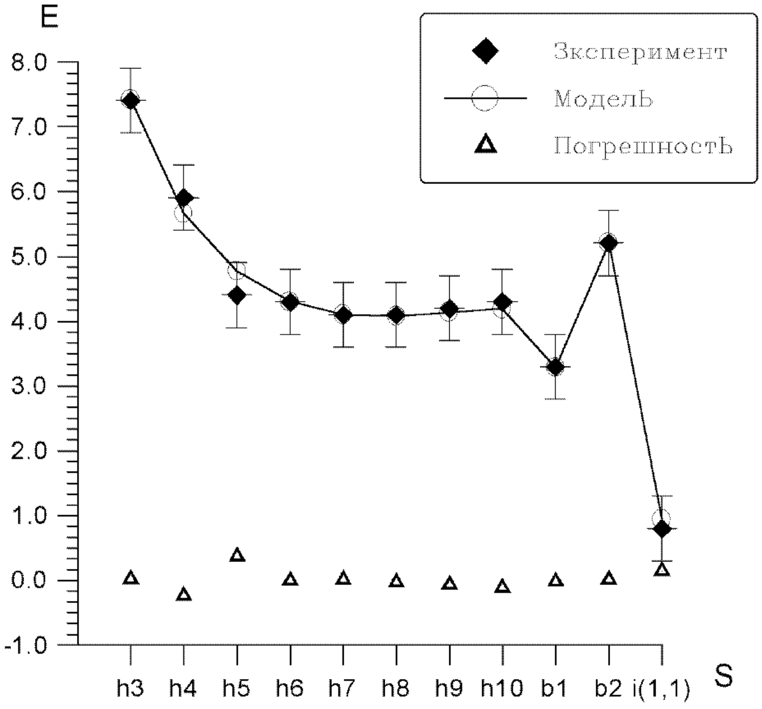

Рис. 8б

Figure 10: Comparison between experimental and model energy (variant 02).